Characterization of the Cu^+ Sites in High-Silica Zeolites Interacting with the CO Molecule: Combined Computational and Experimental Study

Markéta Davidová,[†] Dana Nachtigallová,[†] Roman Bulánek,[‡] and Petr Nachtigall*[,†,‡]

J. Heyrovský Institute of Physical Chemistry, Academy of Sciences of the Czech Republic and Center for Complex Molecular Systems and Biomolecules, Dolejškova 3, 182 23 Prague 8, Czech Republic, and University of Pardubice, Faculty of Chemical Technology, Čs. legií 565, 53210 Pardubice, Czech Republic

Received: September 13, 2002; In Final Form: January 13, 2003

Interactions of the CO molecule with the Cu^+ sites within MFI and FER matrices were investigated by means of the combined quantum mechanics/interatomic potential function method. CO molecules strongly interact with both dominant Cu^+ site types (on the channel wall and on the channel intersection) in high-silica zeolite matrices. Upon interaction with CO, the Cu^+ ion stays coordinated to only two oxygen atoms of the single AlO_4 unit. The structure, coordination, and CO stretching frequencies were found to be very similar for both Cu^+ site types. On the contrary, adsorption energies differ for individual site types. The results are in agreement with the available experimental data, and they were confirmed by the TPD experiments carried out for various zeolite matrices.

1. Introduction

Characterization of the copper/zeolite systems attracts much attention from both experimentalists and theoreticians. Despite the large effort over the last few years, the details of the coordination environment of Cu^+ ions are not fully understood. Knowledge of the details of the structure and coordination of copper ions in high-silica zeolites is essential for understanding the mechanism of deNO_x processes at the atomic scale level.

For the direct decomposition of NO to molecular nitrogen and oxygen, the Cu/MFI system has been shown to have the highest catalytic activity.[1] The catalytic activity of copper ions differs for various zeolite structures, Si/Al ratios, and Cu loading.[2,3] On the basis of numerous experimental studies (employing EXAFS, EPR, IR, UV−vis, and microcalorimetry), it is now generally accepted that two dominant site types exist in high-silica zeolite matrices (see, for example, refs 4−6). On the basis of primarily UV−vis characterization, Dědeček et al. concluded that in MFI the Cu^+ ions preferably occupy sites in the main channel (denoted α) and sites on the deformed six-membered ring on the wall of the zigzag channel (denoted β) in the vicinity of one and two AlO_4 tetrahedra, respectively.[4] Using a combination of EXAFS and UV−vis techniques, Lamberti et al. found two- and three-coordinated Cu^+ sites in MFI.[5] With a combination of EXAFS and microcalorimetry, Kumashiro et al. showed that two dominant Cu^+ sites in MFI are characterized by different CO adsorption energies.[6]

Often, the CO molecule was used as a probe in characterizing the Cu^+ sites in zeolites.[5−18] CO strongly interacts with Cu^+ ions inside the zeolite matrix, forming mono-, di-, and even tricarbonyl species.[9] IR bands in the range of 2129−2164 cm^{-1} (2157−2159 cm^{-1} for MFI) were assigned to the CO stretching mode of monocarbonyl. Some authors deconvoluted this band into two peaks (2151 and 2159 cm^{-1} for MFI) and assigned them to different Cu^+ sites (for example, see refs 6 and 11). The CO stretching band observed for Cu^+/zeolite systems is blue-shifted with respect to the frequency of CO in the gas phase. Using an EXAFS experiment, Kumashiro et al. and Lamberti et al. showed that Cu^+ coordination to framework oxygen atoms is lowered upon the adsorption of the CO molecule.[6,9]

The CO/Cu/zeolite system was also investigated computationally, employing small cluster models.[19−21] Treesukol et al. used the electrostatic embedding approach to describe the CO interaction with the Cu^+ site on the channel intersection in MFI.[22] The interaction of copper ions with the MFI and FER frameworks was studied previously in our laboratory by means of the combined QM-pot technique.[23−25] Two dominant types of Cu^+ ion sites were identified in both zeolite frameworks. Sites where the Cu^+ ions are coordinated to three or four oxygen atoms of the six-membered ring on the wall of one of the channels are denoted "type I" sites. Sites where the Cu^+ ions are coordinated to only two oxygen atoms of the AlO_4 tetrahedron located on the channel intersection are denoted "type II" sites (Figure 1).

In this contribution, we present the results of the combined quantum mechanical/interatomic potential function (QM-pot)[26,27] study of the CO interaction with copper sites in high-silica zeolites (MFI and FER) together with TPD spectra of CO adsorbed in various high-silica zeolite matrices. The computational and experimental details are given in sections 2.1 and 2.2, respectively. Results are reported in section 3, and the discussion, including a comparison with relevant experimental results, is given in section 4.

2.1. Calculations

The structures of CO molecules adsorbed on the Cu^+ sites in MFI and FER frameworks were obtained by energy minimization using the QM-pot technique.[27] Within this approach, the CO/Cu/MFI was represented by a unit cell consisting of 96 T atoms (1 or 2 Al atoms and 95 or 94 Si atoms, respectively), 192 framework oxygen atoms, a copper ion, and a CO molecule. A unit cell consisting of 72 T atoms (1 Al atom and 71 Si atoms), 144 oxygen atoms, copper, and a CO molecule

* Corresponding author. E-mail: petr.nachtigall@jh-inst.cas.cz.
[†] Academy of Sciences of the Czech Republic and Center for Complex Molecular Systems and Biomolecules.
[‡] University of Pardubice.

10.1021/jp026989o CCC: $25.00
Published on Web 02/15/2003

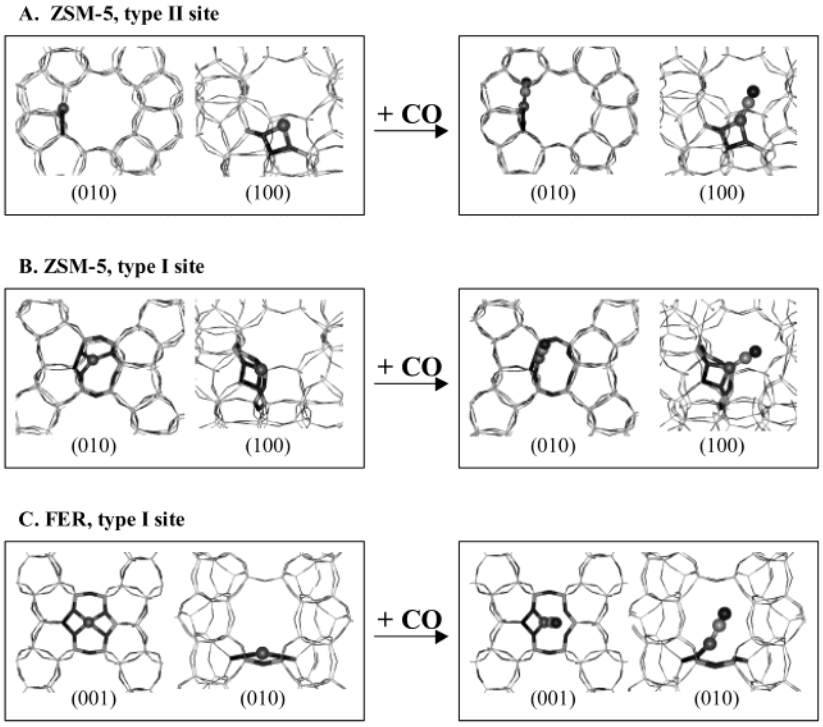

Figure 1. Cu^+ sites in MFI and FER. The structures without and with the adsorbed CO molecule are depicted in the left and right panels, respectively. Type I and type II sites are located on the channel wall and on the channel intersection, respectively. For each structure, a view along the main channel ((010) and (001) cut for MFI and FER, respectively) and a view along the perpendicular channel ((100) and (010) cut for MFI and FER, respectively) are shown.

represented the CO/Cu/FER system. The periodic boundary conditions were applied to the unit cell. Part of the unit cell ("inner" part) including the CO molecule, Cu^+, and the surrounding zeolite framework atoms was treated at the DFT level, employing the B3LYP exchange-correlation functional.[28,29] The dangling bonds of the inner part were saturated by H atoms connected to framework oxygen atoms. The sizes of the inner part ranging from three to nine TO_4 units (from $CO-CuT_3O_2(OH)_8$ to $CO-CuT_9O_{11}(OH)_{14}$), depending on the type of the Cu^+ site, were considered. A valence double-ζ-plus-polarization function basis set was used on Cu, Si, Al, and H atoms, and a valence triple-ζ-plus-polarization function basis set was used on O and C atoms.[30,31] The interaction between atoms from the inner part and other atoms in the system and the interactions between atoms outside the inner part were described at the interatomic potential function (IPF) level. The core−shell model potential[32] was used for the description of the zeolite framework (parameters taken from ref 33) and the description of the Cu^+ interaction with the framework (parameters taken from ref 23). The interaction between the CO molecule and the zeolite framework was described with the Lennard-Jones potential with parameters derived from the universal force field.[34] The interatomic potential function for the interaction of the CO molecule with the Cu^+ ions was not defined since these atoms were always inside the inner part of the system treated at the DFT level.

The binding energies of the CO molecules to the Cu^+/zeolite were calculated as follows:

$$\text{Cu(I)/zeolite} + \text{CO} \rightarrow \text{(CO)Cu(I)/zeolite} \qquad (1)$$

The calculations were carried out with the QM-pot program,[27] which makes use of the TurboDFT[35] and GULP[36] programs for DFT and IPF calculations, respectively.

The interaction of carbon monoxide with the Cu^+ ions is relatively well described at the level of theory used in this paper.

TABLE 1: Interaction Energies for the Process $CO + Cu^+(CO)_{n-1} \rightarrow Cu^+(CO)_n$, $n = 1-4$

	interaction energies (kcal/mol)	
n(CO)	B3LYP/VD(T)ZP[a]	experiment[b]
1	−39	−36
2	−37	−41
3	−17	−18
4	−15	−13

[a] Including the zero-point energy correction. [b] From ref 57.

This is documented in Table 1, where the experimental interaction energies of one to four CO molecules with Cu^+ are compared with calculated energies. All four sequential bond energies calculated at the B3LYP level differ from experiment at most by 4 kcal/mol.

Vibrational analysis was carried out within the harmonic approximation at the combined quantum mechanic/interatomic potential function level.

The interaction of a carbon monoxide molecule with the Cu^+ ions was investigated for type I and type II sites of copper in both MFI and FER matrices. For the interaction with copper at the type I site in MFI, the six-membered ring on the wall of the zigzag channel ("Z6" according to the notation introduced in ref 23) was used with the Al atom at the T4 position. The interaction of CO with Cu^+ in the vicinity of two Al atoms was studied on the same ring with Al atoms placed in T4 and T10 positions and the proton located on the oxygen atom of the T10 tetrahedron. (For T sites, we use the numbering scheme introduced for orthorhombic symmetry by Koningsveld.[37]) The type I site in FER was represented by a six-membered ring on the wall of the perpendicular channel ("P6" according to the notation introduced in ref 24) with the Al atom in the T1 site. (The T-site numbering of ref 38 was adopted.) For type II sites on the intersection of two channels, the aluminum atom was placed either on the T12 or T6 position in MFI or on the T2 or

TABLE 2: Chemical Composition of Zeolite Samples and Ion-Exchange Parameters

sample[a]	original zeolite	T (K)	solution	time (h)
CuNa−MFI−14.1−0.19−1.13	Na−MFI	298	0.01 M $Cu(Ac)_2$	12
CuNaK−FER−8.5−0.25−2.18	NaK−FER	298	0.001 M $Cu(Ac)_2$	24
CuNaK−FER−8.5−0.13−1.10	NaK−FER	298	0.0002 M $Cu(Ac)_2$	24
CuNaK−ERI−3.6−0.11−1.79	NaK−ERI	333	0.01 M $CuCl_2$	4

[a] Notation used: copper−co-cation−zeolite topology−Si/Al molar ratio−Cu/Al molar ratio−weight % of copper.

T4 position in FER. The Cu^+ site types considered in this study are depicted at Figure 1.

2.2. Experimental Section

Cu−Zeolite Preparation. The preparation of the Cu/zeolite samples was described in detail in ref 18. The chemical compositions were determined by wavelength-disperse X-ray fluorescence spectroscopy (WD XRF) and by atomic absorption spectroscopy after the dissolution. A gravimetric method was used for the Si content determination. Conditions of the preparation of zeolites and their chemical compositions are given in Table 2. Throughout this paper, the following notation for the samples is used: copper−co-cation−zeolite topology−Si/Al molar ratio−Cu/Al molar ratio−weight % of copper (e.g., CuNa−MFI−14.1−0.19−1.13).

CO TPD Experiment. TPD experiments were carried out in the quartz microreactor loaded with 100 mg of the zeolite sample. The TPD apparatus was equipped with an OmniStar GDS 300 quadrupole mass spectrometer. Mass fractions at 4, 12, 14, 18, 28, and 44 were monitored simultaneously during the TPD experiment. The intensities of the individual mass fractions were registered every 3 s.

Samples were calcined in a flow of oxygen at 450 °C for 2 h and reduced by a gas mixture consisting of 95 vol % of He and 5 vol % of CO prior to the TPD experiment. The total flow rate of the reduction gas was 25 $cm^3\ min^{-1}$, and the temperature increased with heating rate of 10 °C min^{-1} from 25 to 450 °C. The samples were cooled in a flow of reduction gas to room temperature after the reduction and subsequently flushed with He at flow rate 30 $cm^3\ min^{-1}$. When the mass intensity of the species monitored by Omnistar became constant, the temperature was ramped to 600 °C at a heating rate of 10 °C min^{-1}.

3. Results

3.1. Interaction of the CO Molecule with Cu^+/Zeolite. Carbon monoxide interacts strongly with both types of Cu^+ sites in the MFI and FER matrices. The coordination numbers of the Cu^+ ions with the zeolite framework, bond lengths, angles, binding energies, and C−O stretching frequencies are summarized in Table 3. Upon the interaction with the CO molecule, the Cu^+ ion stays coordinated to only two oxygen atoms of the AlO_4 tetrahedron, and the coordination of the Cu^+ ions with the zeolite framework is very similar for both zeolites and for both Cu^+ site types (Figure 1). The C−O bond lengths are within 1.131−1.134 Å for all Cu^+ sites. The CO molecule is always bonded to the Cu^+ ion in a direction where it can reach the open space at the channel intersection. The sp hybridization on the carbon atom requires a linear Cu−C−O structure and a planar coordination of two framework O atoms, and the carbon atom of the CO molecule on the Cu^+ ion is preferable. Such coordination can be easily reached for the Cu^+ ions located on the intersection of two channels (type II sites) without significant changes in the [Cu^+−zeolite] interaction. Therefore, the interaction of the CO molecule with the Cu^+ ion in type II sites leads to only very small changes in Cu−O distances, and the coordination of copper with the zeolite framework does not change at all (Figure 1, part A). Upon interactions with single CO molecules, the Cu−O bond lengths are within 0.02 Å of their original values (except one site where Cu^+ binds to framework oxygen atoms in a rather nonsymmetrical way, with Cu−O distances of 2.01 and 2.16 Å). On the contrary, the CO molecule cannot bind to Cu^+ ions on the channel wall (type I sites) without major changes in the [Cu^+−zeolite] coordination (Figure 1, parts B and C). For these sites, the Cu^+ ions are lifted farther from the channel wall, and they lose their coordination to non-AlO_4 oxygen atoms.

A partial loss of the Cu^+ coordination observed for type I sites corresponds to the decrease in the CO adsorption energy. The interaction energies of CO with zeolite were found to be below 36 kcal/mol and over 40 kcal/mol for type I and type II sites, respectively (Table 3). We can formally divide the adsorption process (1) into two steps:

$$\text{Cu(I)/zeolite} \rightarrow [\text{Cu(I)/zeolite}]^{\neq} \quad (2a)$$

$$[\text{Cu(I)/zeolite}]^{\neq} + (\text{CO})_g \rightarrow (\text{CO})\text{Cu(I)/zeolite} \quad (2b)$$

where $[\text{Cu(I)/zeolite}]^{\neq}$ denotes the hypothetical system where the Cu^+ ion is located at the optimal geometry for the interaction with the CO molecule. Thus, eq 2a defines the lattice relaxation energy that has to be given to the system in order to bind carbon monoxide efficiently. The relaxation energy is less than 2 kcal/mol for all type II sites considered in this study, but it is 6−12

TABLE 3: Calculated Cu^+ Coordination Numbers, Structure Parameters, Binding Energies, and CO Stretching Vibrations

	type	Al site	CN_o[a]	CN_z[b]	R(Cu−O)[c] (Å)	R(Cu−O)[d] (Å)	Θ(Cu−C−O)[e]	Bζ-OcuO−CO[f]	E_b (kcal/mol)	$\tilde{\nu}$ (cm^{-1})
MFI	II	T12[g]	2	2	2.04, 2.05	2.04, 2.06	179	179	−42	2198
	II	T12[h]	2	2	2.06, 2.07	2.05, 2.08	179	175	−42	2205
	II	T6[i]	2	2	2.05, 2.06	2.03, 2.05	178	176	−42	2195
	II	T6[j]	2	2	2.05, 2.07	2.01, 2.16	177	165	−44	2207
	I	T4	3	2	2.08, 2.14, 2.13	2.06, 2.06	179	175	−36	2205
	I	T4, T10	3	2	2.00, 2.01, 2.21	2.04, 2.05	179	174	−29	2207
FER	II	T2	2	2	2.05, 2.08	2.05, 2.07	176	171	−40	2200
	II	T4	2	2	2.06, 2.08	2.03, 2.10	171	156	−37	2202
	I	T1	4	2	2.06, 2.14, 2.12, 2.44	2.10, 2.12	179	161	−27	2211
	I	T1,T1	4	2	2.08, 2.12, 2.17, 2.31	2.15, 2.16, 2.54, 2.63	179	145	−24	2212

[a] Number of oxygen atoms in coordination with Cu^+ (atoms closer than 2.5 Å are considered) before the adsorption of CO (refs 23 and 24). [b] Number of oxygen atoms in coordination with the Cu^+ ion after the adsorption of CO. [c] Cu−O bond distances correspond to structures before the CO adsorption (refs 23 and 24). [d] Cu−O bond distances correspond to structures after the CO adsorption. [e] (Cu−C−O) bond angle. [f] Angle between the CO molecule and the plane defined by the Cu atom and the two O atoms in coordination with Cu. [g] T12−T12−T3 fragment of MFI considered. [h] T12−T11−T3 fragment of MFI considered. [i] T9−T6−T5 fragment of MFI considered. [j] T9−T6−T2 fragment of MFI considered.

TABLE 4: TPD Peak Characteristics

zeolite[a]	peak area[b] W_{Cu}(wt %)	peak maxima[c] A	peak maxima[c] B	desorption end[c]	relative peak area (%) A	relative peak area (%) B
CuNaK−ERI−3.6−0.11−1.79	1.4953	196		294	100	
CuNaK−FER−8.5−0.13−1.10	1.467	190	271	335	83.2	16.8
CuNaK−FER−8.5−0.25−2.18	1.4622	186	298	400	57.2	42.8
CuNa−MFI−14.1−0.19−1.13	1.2265	175	342	429	13.2	86.8

[a] Notation used: copper−co-cation−zeolite topology−Si/Al molar ratio−Cu/Al molar ratio−weight % of copper. [b] Overall peak area devided by the copper weight percentage in the sample. [c] In °C.

kcal/mol for type I sites. The interaction of CO with the Cu^+ ion in the zeolite with the optimal geometry for the CO/Cu/zeolite system (defined by eq 2b) is very similar for all Cu^+ sites.

All CO stretching frequencies summarized in the last column of Table 3 fall in the range of 2198−2211 cm^{-1}. This is about 50 cm^{-1} more than the experimentally measured frequency of 2157−2159 cm^{-1}.[6,11−14,17,18,39,40] Part of the error is due to the harmonic approximation used in our calculations (the anharmonic correction for the gas-phase CO stretch is about −27 cm^{-1}),[41] and the rest is due to the deficiency of the model and method employed. An empirical scaling factor is often used to get calculated frequencies into better agreement with experimental values.[42] We are rather interested in relative stretching frequencies for CO coordinated to the Cu^+ ions at various sites in various zeolite matrices; therefore, the frequencies reported in Table 3 are not corrected with any scaling factor. All calculated stretching frequencies are very similar for both site types considered and also for both MFI and FER.

Comparing the CO interaction with Cu^+ in the type I site in the vicinity of one or two AlO_4 tetrahedra reveals that the second AlO_4 unit in the vicinity of the Cu^+ ion does not have any influence on the resulting structure. The coordination numbers, geometrical parameters, and CO stretching frequencies are almost identical. (See Table 3.) However, the coordination changes observed upon the CO adsorption described above are energetically more demanding because of the stronger binding of the Cu^+ ion to the zeolite framework in the vicinity of two AlO_4 tetrahedra. This corresponds to a smaller binding energy of CO to sites where Cu^+ is coordinated to two AlO_4 tetrahedra compared to those where Cu^+ is coordinated to the ring containing only a single AlO_4 tetrahedron.

3.2. TPD Experiment. A series of TPD experiments of CO adsorbed on various zeolite matrices differing in their Si/Al ratios and copper content were carried out. The TPD spectra of CO measured for MFI, FER, and ERI are presented in Figure 2, and the peak temperatures and relative peak areas are summarized in Table 4. With the exception of ERI, all TPD spectra have two desorption peaks, the lower-temperature peak (A) having maximum around 190 °C and the higher-temperature peak (B) having maximum above 275 °C. Peaks A and B are well separated, and the overall peak area agrees well with the Cu^+ content. (See the second column of Table 4.) The TPD spectrum of Cu^+/ERI (spectrum a in Figure 2) shows only peak A. In both TPD spectra measured for Cu^+/FER (spectra b and c in Figure 2 for samples with lower and higher copper content, respectively), low-temperature peak A is dominant. The relative size of peak A is greater for the sample with lower copper content (relative peak area 83%) than for the sample with higher copper content (relative peak area 57%). On the contrary, the TPD spectrum of Cu^+/MFI (spectrum d) shows a dominant high-temperature peak (87%).

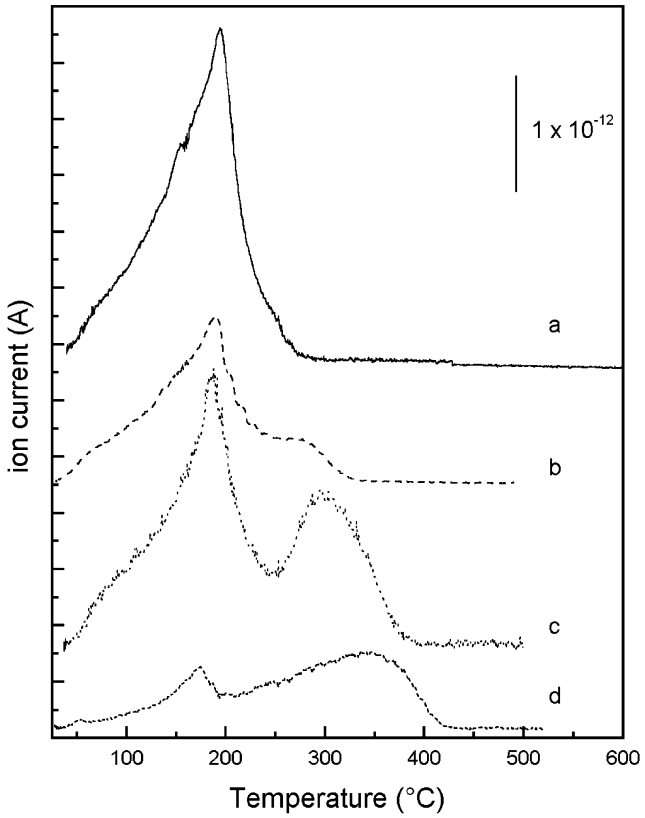

Figure 2. CO TPD profiles of Cu−zeolites reduced in a CO gas mixture and saturated by CO at 25 °C. (a) CuNa−ERI−3.6−0.08−1.29, (b) CuNaK−FER−8.5−0.25−1.10, (c) CuNaK−FER−8.5−0.13−2.18, (d) CuNa−MFI−14.1−0.19−1.13. (For notation, see Table 2.)

4. Discussion

Calculated changes in the Cu^+ ion interaction with the zeolite framework upon CO adsorption are in agreement with numerous experimental findings. Zecchina et al. found that all Cu^+ sites in MFI are accessible to CO,[43] contrary to other matrices, faujasite,[44] and mordenite[45] in particular. Sarkany observed the frequency shift of the zeolite asymmetric stretching vibration due to the interaction with $Cu^+(CO)_n$ species.[46] The asymmetric stretching vibration at 968 cm^{-1} observed in the presence of Cu^+(CO) species in MFI was attributed to an increased Cu−O distance and a decrease in the Cu−O force constant by Zecchina et al.[43] This interpretation was confirmed by the results of XAFS experiments for di- and tricarbonyl species in Cu/MFI.[9]

Using the XAFS technique, Kumashiro et al. also found changes in the Cu^+ coordination environment upon adsorption of CO.[6] The average Cu−C distance of 1.89 Å was found, and the average distance between Cu^+ and framework oxygen atoms increases from 1.98 to 2.05 Å when CO is adsorbed. Using a combination of XAFS, IR, electron spectroscopy, and adsorption calorimetry techniques, Kumashiro et al. concluded that two

types of Cu^+ sites differing in CO adsorption energy can be distinguished in MFI: (i) a strongly interacting Cu^+ site (Δ_{ads} = 29 kcal/mol) characterized by a 2159-cm^{-1} stretching band where the Cu^+ ion is coordinated to two framework oxygen atoms and (ii) a Cu^+ site (Δ_{ads} = 24 kcal/mol) characterized by a 2151 cm^{-1} band where the Cu^+ ion is coordinated to three framework oxygen atoms.

In agreement with these results, our study also predicts the existence of two Cu^+ site types differing in their CO adsorption energy and Cu^+ coordination environment. However, we were not able to associate either of these two sites with a distinct CO stretching band. The calculated frequencies corresponding to the CO stretch for CO adsorbed on type I and type II sites of Cu^+ in MFI are in the ranges of 2205−2207 and 2198−2207 cm^{-1}, respectively. For CO adsorbed in FER, the calculated CO stretching frequencies are in the ranges of 2211−2212 and 2198−2202 cm^{-1} for type I and type II sites, respectively. Two bands in FER appear to be distinguished; however, a higher-energy band is found for the type I site, where CO has a lower adsorption energy and where the Cu^+ ion is coordinated to three to four framework oxygen atoms prior to CO adsorption. This contradicts the results of Kumashiro et al., who assigned the higher-energy band to the site with the higher CO adsorption energy and lower Cu^+ coordination. The calculations of small vibrational frequency shifts are certainly more complicated and less reliable than the calculations of interaction energies or structural parameters. Therefore, we conclude that present calculations are not able to provide CO stretching frequencies reliably enough to assign two overlapping IR bands at 2159 and 2151 cm^{-1}. Some authors did not split the 2158 cm^{-1} band into two peaks (e.g., see refs 13, 14, and 17). Using diffuse reflectance FTIR, Borovkov et al. analyzed fundamental, combination, and overtone vibrations of adsorbed CO and concluded that two types of Cu^+ sites can hardly be discriminated by IR spectroscopy.[40] Recent results of a TPD-IR study of CO desorption from Cu^+/MFI shows that a higher-energy stretching band may correspond to a lower CO adsorption energy site,[47] contrary to the results of Kumashiro et al.

Making reliable calculations of the CO stretching frequencies for CO adsorbed on Cu^+ is a computationally difficult task. Experimentally, it was clearly shown that the CO stretching frequency shows a blue shift upon the adsorption on Cu^+ sites in zeolites. The majority of theoretical studies failed to reproduce this blue shift (e.g., see ref 21). Only when very poor models (zeolite framework represented by a few water molecules) were employed was a correct frequency shift for the CO stretch obtained.[19,20] A blue shift was recently obtained by Treesukol et al., who used the electrostatic embedding model.[22] They concluded that for the correct description of the CO stretching frequency shift the effect of the Madelung potential should be taken into consideration. A discussion of the reliability of models for a description of the vibrational spectra of adsorbed molecules is beyond the scope of this paper. Work in this direction is under way in our laboratory.[48] Using the same combined QM-pot scheme, we found the CO stretching frequency blue shift upon the adsorption of the Li^+/MFI system at +48 cm^{-1} to be in excellent agreement with the experimental value[49] (45 cm^{-1}). We believe that the difficulty in describing the CO stretching vibration shift in the Cu^+/MFI system is not due to the importance of the Madelung potential but is due to the overestimation of the back-donation effect at the DFT level employing the B3LYP functional.

As discussed in the previous section, the calculated CO stretching frequencies are in the same range for both Cu^+ site types of the Cu^+ ions; therefore, the assignment of 2159- and 2151-cm^{-1} peaks to different types of Cu^+ sites is not supported by our calculations. Even the presence of two Al atoms on the six-membered ring in coordination with Cu^+ does not change the CO stretching frequencies. However, two types of Cu^+ sites found in MFI and FER show significant differences in binding energies (Table 3), thus individual types of Cu^+ sites should be distinguishable in measurements of adsorption heats or temperature-programmed desorption. Kuroda et al. measured the isothermal heats of adsorption of CO on the Cu/MFI system and found two[50] or even three[6] distinguishable sites.

In the TPD spectra described above, one can clearly identify two distinct peaks. None of the peaks can be due to the presence of dicarbonyl species since dicarbonyl species are completely destroyed by outgassing the sample at RT.[51] In addition, the presence of Na(K) carbonyls should not be important under the experimental conditions.[52,53] On the basis of the results of the calculations presented in section 4.1., we suggest that the lower- and higher-temperature peaks are due to CO desorption from type I (channel wall) and type II (channel intersection) sites of the Cu^+ ions, respectively. This interpretation is supported by the following arguments. It has been found previously[23] that the Cu^+ ions preferentially occupy type II sites in MFI (relatively large peak B in TPD spectra) whereas type I sites are preferentially occupied by Cu^+ ions in FER[24] (peak A is larger than peak B). For the Cu/FER system, it was found previously that sites on the channel intersection can be populated only when sites on the channel wall are filled.[24] This is again in agreement with the relative peak areas summarized in Table 4. The absence of a high-temperature peak in the TPD spectra of ERI (spectra a in Figure 2) corresponds to the presence of only type I sites in this sample.

The experimental determination of the structure and environment of the Cu^+ sites inside the high-silica zeolite matrices is very difficult and relies on indirect (UV−vis, IR) or averaging (EXAFS) techniques. Nevertheless, great progress has been achieved during the past few years: (i) UV−vis in combination with EPR and IR methods led Wichterlova and co-workers to conclude that two Cu^+ site types are dominantly occupied in MFI[4] (α site on the wall of the main channel and β site on top of the deformed six-membered ring on the wall of the zigzag channel). (ii) Using EXAFS in combination with other techniques, Lamberti et al. also found two types of Cu^+ sites[5] (two-coordinated and three-coordinated sites). (iii) With a combination of EXAFS and IR of the probe CO molecule, Kumashiro et al. also found two Cu^+ site types.[6] (Sites with the higher Cu^+ coordination were characterized with the lower adsorption heat of CO and the lower CO stretching frequency.) These results can be compared with the results of the present study: calculations of excitation and emission spectra for Cu^+ in MFI and FER showed that the α and β sites of Wichterlova are the sites on the channel intersection (type II) and the sites on the channel wall (type I), respectively.[24,54] The two- and three-coordinated sites found by Lamberti et al. correspond to sites on the channel intersection and on the channel wall, respectively.[23] The type I and type II sites of Cu^+ differ in their interaction energies of CO, in agreement with the results of Kumashiro et al. The results of the combined QM-pot study are in agreement with experimental data and give us new information about the structure and environment of the Cu^+ ions inside the high-silica zeolite matrices. Similar changes in the Cu^+ ion interaction were previously reported for the NO molecule interaction with the Cu^+/MFI system.[55,56]

5. Conclusions

The results of the combined QM-pot study show that two different Cu^+ site types identified in high-silica zeolite matrices become very similar upon the interaction with the single molecule of carbon monoxide. The overall coordination number for Cu^+ is 3 (2 framework oxygen atoms and a carbon atom of CO) for all of the structures that were considered. The geometrical parameters and vibrational frequencies are also very similar for both Cu^+ site types. The CO adsorption energies are larger for the sites on the intersection than for the sites on the channel wall. For the Cu^+ sites on the intersection, there is almost no change in the coordination of the Cu^+ ions with the zeolite framework upon interaction with CO. On the contrary, for the Cu^+ sites on the channel wall, the Cu^+ ion partially loses its coordination with the zeolite framework upon interaction with CO. A partial loss of Cu^+ coordination corresponds to smaller adsorption energies of CO at these sites. To bind CO efficiently, the Cu^+ ion must be lifted farther from the channel wall, thus decreasing the $Cu^+\cdots$zeolite framework interaction. Calculated differences in CO adsorption energies are in good agreement with available experimental data and with the results of the TPD study. There are only small differences between the Cu^+ sites on the channel intersection of MFI and FER. However, the sites on the channel wall of MFI and FER differ by almost 10 kcal/mol in CO interaction energies. The interaction energy of CO with the Cu^+ sites is smaller when Cu^+ is located on top of the six-membered ring consisting of two AlO_4 tetrahedra. On the basis of the results of the QM-pot study, the two types of Cu^+ sites could not be distinguished by the CO stretching frequency.

Acknowledgment. This work has been supported by a grant from the Czech Ministry of Education to the Center for Complex Molecular Systems and Biomolecules (LN00A032). P.N. also acknowledges support from the Granting Agency of the Czech Republic (grant no. 203/00/0637). We thank J. Sauer for helpful discussions and B. Wichterlova for helpful discussions and for reading the manuscript. Thanks go also to Marek Sierka, who wrote the QM-pot code.

References and Notes

(1) Iwamoto, M.; Furukawa, H.; Mine, Y.; Uemura, F.; Mikuriya, S.; Kagawa, S. *J. Chem. Soc., Chem. Commun.* **1986**, 1272.
(2) Wichterlova, B.; Dedecek, J.; Sobalik, Z.; Vondrova, A.; Klier, K. *J. Catal.* **1997**, *169*, 194.
(3) Moretti, G. *Catal. Lett.* **1994**, *23*, 135.
(4) Dedecek, J.; Sobalik, Z.; Tvaruzkova, Z.; Kaucky, D.; Wichterlova, B. *J. Phys. Chem.* **1995**, *99*, 16327.
(5) Lamberti, C.; Bordiga, S.; Salvalaggio, M.; Spoto, G.; Zecchina, A.; Geobaldo, F.; Vlaic, G.; Bellatreccia, M. *J. Phys. Chem. B* **1997**, *101*, 344.
(6) Kumashiro, P.; Kuroda, Y.; Nagao, M. *J. Phys. Chem. B* **1999**, *103*, 89.
(7) Palomino, G. T.; Bordiga, S.; Zecchina, A.; Marra, G. L.; Lamberti, C. *J. Phys. Chem. B* **2000**, *104*, 8641.
(8) Bordiga, S.; Paze, C.; Berlier, G.; Scarano, D.; Spoto, G.; Zecchina, A.; Lamberti, C. *Catal. Today* **2001**, *70*, 91.
(9) Lamberti, C.; Palomino, G. T.; Bordiga, S.; Berlier, G.; D'Acapito, F.; Zecchina, A. *Angew. Chem., Int. Ed.* **2000**, *39*, 2138.
(10) Bolis, V.; Maggiorini, S.; Meda, L.; D'Acapito, F.; Palomino, G. T.; Bordiga, S.; Lamberti, C. *J. Chem. Phys.* **2000**, *113*, 9248.
(11) Kuroda, Y.; Yoshikawa, Y.; Kumashiro, R.; Nagao, M. *J. Phys. Chem. B* **1997**, *101*, 6497.
(12) Kuroda, Y.; Kumashiro, R.; Itadani, A.; Nagao, M.; Kobayashi, H. *Phys. Chem. Chem. Phys.* **2001**, *3*, 1383.
(13) Chen, H. Y.; Chen, L.; Lin, J.; Tan, K. L.; Li, J. *Inorg. Chem.* **1997**, *36*, 1417.
(14) Szanyi, J.; Paffett, M. T. *Catal. Lett.* **1997**, *43*, 37.
(15) Milushev, A.; Hadjiivanov, K. *Phys. Chem. Chem. Phys.* **2001**, *3*, 5337.
(16) Hadjiivanov, K.; Knozinger, H. *J. Catal.* **2000**, *191*, 480.
(17) Hadjiivanov, K. I.; Kantcheva, M. M.; Klissurski, D. G. *J. Chem. Soc., Faraday Trans.* **1996**, *92*, 4595.
(18) Bulanek, R.; Wichterlova, B.; Sobalik, Z.; Tichy, J. *Appl. Catal., B* **2001**, *31*, 13.
(19) Ramprasad, R.; Schneider, W. F.; Hass, K. C.; Adams, J. B. *J. Phys. Chem. B* **1997**, *101*, 1940.
(20) Brand, H. V.; Redondo, A.; Hay, P. J. *J. Phys. Chem. B* **1997**, *101*, 7691.
(21) Trout, B. L.; Chakraborty, A. K.; Bell, A. T. *J. Phys. Chem.* **1996**, *100*, 17582.
(22) Treesukol, P.; Limtrakul, J.; Truong, T. N. *J. Phys. Chem. B* **2001**, *105*, 2421.
(23) Nachtigallova, D.; Nachtigall, P.; Sierka, M.; Sauer, J. *Phys. Chem. Chem. Phys.* **1999**, *1*, 2019.
(24) Nachtigall, P.; Davidova, M.; Nachtigallova, D. *J. Phys. Chem. B* **2001**, *105*, 3510.
(25) Nachtigallova, D.; Nachtigall, P.; Sauer, J. *Phys. Chem. Chem. Phys.* **2001**, *3*, 1552.
(26) Eichler, U.; Kolmel, C. M.; Sauer, J. *J. Comput. Chem.* **1997**, *18*, 463.
(27) Sierka, M.; Sauer, J. *J. Chem. Phys.* **2000**, *112*, 6983.
(28) Becke, A. D. *J. Chem. Phys.* **1993**, *98*, 5648.
(29) Lee, C.; Yang, W.; Parr, F. G. *Phys. Rev. B: Condens. Matter* **1988**, *37*, 785.
(30) Schafer, A.; Horn, H.; Ahlrichs, R. *J. Chem. Phys.* **1992**, *97*, 2571.
(31) Rodriguez-Santiago, L.; Sierka, M.; Branchadell, V.; Sodupe, M.; Sauer, J. *J. Am. Chem. Soc.* **1998**, *120*, 1545.
(32) Dick, B. G.; Overhauser, A. W. *Phys. Rev.* **1958**, *112*, 90.
(33) Sierka, M.; Sauer, J. *Faraday Discuss.* **1997**, 41.
(34) Rappe, A. K.; Casewit, C. J.; Colwell, K. S.; Goddard, W. A.; Skiff, W. M. *J. Am. Chem. Soc.* **1992**, *114*, 10024.
(35) Treutler, O.; Ahlrichs, R. *J. Chem. Phys.* **1995**, *102*, 346.
(36) Gale, J. D. *J. Chem. Soc., Faraday Trans.* **1997**, *93*, 629.
(37) Koningsveld, H. v.; Jansen, J. C.; Bekkum, H. v. *Acta Crystallogr.* **1987**, *7*, 564.
(38) Vaughan, P. A. *Acta Crystallogr.* **1966**, *21*, 983.
(39) Lamberti, C.; Salvalaggio, M.; Bordiga, S.; Geobaldo, F.; Spoto, G.; Zecchina, A.; Vlaic, G.; Bellatreccia, M. *J. Phys. IV* **1997**, *7*, 905.
(40) Borovkov, V. Y.; Jiang, M.; Fu, Y. L. *J. Phys. Chem. B* **1999**, *103*, 5010.
(41) Mantz, A. W.; Maillard, J. P. *J. Mol. Spectrosc.* **1975**, *57*, 155.
(42) Scott, A. P.; Radom, L. *J. Phys. Chem.* **1996**, *100*, 16502.
(43) Zecchina, A.; Bordiga, S.; Palomino, G. T.; Scarano, D.; Lamberti, C.; Salvalaggio, M. *J. Phys. Chem. B* **1999**, *103*, 3833.
(44) Lamberti, C.; Spoto, G.; Scarano, D.; Paze, C.; Salvalaggio, M.; Bordiga, S.; Zecchina, A.; Palomino, G. T.; Dacapito, F. *Chem. Phys. Lett.* **1997**, *269*, 500.
(45) Lamberti, C.; Bordiga, S.; Zecchina, A.; Salvalaggio, M.; Geobaldo, F.; Arean, C. O. *J. Chem. Soc., Faraday Trans.* **1998**, *94*, 1519.
(46) Sarkany, J. *J. Mol. Struct.* **1997**, *410*, 95.
(47) Datka, J.; Kozyra, P. *Stud. Surf. Sci. Catal.* **2002**, *142*, 445.
(48) Bludsky, O.; Silhan, M.; Nachtigall, P. *J. Chem. Phys.* **2002**, *117*, 9298.
(49) Zecchina, A.; Bordiga, S.; Lamberti, C.; Spoto, G.; Carnelli, L.; Arean, C. O. *J. Phys. Chem.* **1994**, *98*, 9577.
(50) Kuroda, Y.; Kumashiro, R.; Yoshimoto, T.; Nagao, M. *Phys. Chem. Chem. Phys.* **1999**, *1*, 649.
(51) Spoto, G.; Zecchina, A.; Bordiga, S.; Ricchiardi, G.; Martra, G.; Leofanti, G.; Petrini, G. *Appl. Catal., B* **1994**, *3*, 151.
(52) Garrone, E.; Fubini, B.; Bonelli, B.; Onida, B.; Arean, C. O. *Phys. Chem. Chem. Phys.* **1999**, *1*, 513.
(53) Savitz, S.; Myers, A. L.; Gorte, R. J. *Microporous Mesoporous Mater.* **2000**, *37*, 33.
(54) Nachtigall, P.; Nachtigallova, D.; Sauer, J. *J. Phys. Chem. B* **2000**, *104*, 1738.
(55) Sauer, J.; Nachtigallová, D.; Nachtigall, P. Ab Initio Simulation of Cu-Species in Zeolites: Siting, Coordination, UV−vis Spectra and Reactivity. In *Catalysis by Unique Metal Ion Structures in Solid Matrices: From Science to Application*; Centi, G., Wichterlová, B., Bell, A. T., Eds.; Kluwer Academic Publishers: Dordrecht, The Netherlands, 2001; Vol. 13, p 221.
(56) Nachtigall, P.; Nachtigallová, D.; Davidova, M.; Sauer, J., to be submitted for publication.
(57) Meyer, F.; Chen, Y. M.; Armentrout, P. B. *J. Am. Chem. Soc.* **1995**, *117*, 4071.